IEEE Access
Multidisciplinary ⋮ Rapid Review ⋮ Open Access Journal

Received 22 February 2023, accepted 15 March 2023, date of publication 20 March 2023, date of current version 23 March 2023.

Digital Object Identifier 10.1109/ACCESS.2023.3258978

RESEARCH ARTICLE

Broadband Spatial Spectrum Estimation Based on Space-Time Minimum Variance Distortionless Response and Frequency Derivative Constraints

YANG WANG, HAIYUN XU, BIN WANG, AND MINGLEI SUN
Information Systems Engineering, PLA Strategic Support Force Information Engineering University, Zhengzhou 450001, China
Corresponding author: Bin Wang (commutech@163.com)

ABSTRACT The two-dimensional optimization capability of the space-time minimum variance distortionless response (STMVDR) can improve the spatial spectrum estimation performance of the broadband beamformer with limited samples, but its high sensitivity to frequency errors may lead to the suppression of some narrowband signals not at the grid point of the frequency spectrum calculation. In order to reduce the sensitivity of STMVDR to frequency errors, a broadband spatial spectrum estimation method based on STMVDR and frequency derivative constraints is proposed in this paper. First, based on the beam response of the STMVDR beamformer, an arbitrary order frequency derivative constraint is derived. Second, combining the gain constraint and frequency derivative constraint, the linear constrained minimum variance problem is established to solve the optimal weight of the beamformer. Finally, the calculation method of the broadband spatial spectrum is derived. Numerical simulations show that the proposed method not only solves the problem of frequency mismatch caused by the insufficient number of points for calculating frequency spectrum, but also does not cause the spatial spectrum peaks to deviate from the true direction due to the broadening of the main lobe of frequency spectrum. In addition, the proposed method can reduce the computational complexity of the algorithm by more than half by increasing the interval of the frequency calculation grid points, and does not significantly loss in the angular resolution capability and estimation accuracy of the algorithm.

INDEX TERMS Space-time minimum variance distortionless response, frequency derivative constraint, broadband spatial spectrum estimation.

I. INTRODUCTION

Spatial spectrum estimation is an important research topic, which is widely used in passive sonar, radar, wireless communication and other fields [1]. Broadband spatial spectrum estimation methods can be divided into space-frequency methods and space-time methods according to different processing domains.

Space-frequency method usually decomposes the time-domain wideband signal into a set of frequency-domain narrowband signals with the help of FFT (Fast Fourier Transform), and then uses narrowband method to estimate Spatial Spectrum [2]. Two classical space-frequency methods are incoherent signal subspace method [3] and coherent signal subspace method [4]. The space-frequency method can obtain accurate spatial spectrum estimation only when the subband bandwidth meets the narrowband condition. Therefore, a large number of time-domain data samples are needed to ensure frequency resolution and sufficiently small subband frequency interval. However, when the sampling time is limited (such as the interference of mobile interference sources or short-time burst signals), the narrow-band filtering in space-frequency method has serious leakage of spectral energy. The spectral leakage will cause the peak to deviate from the true direction in the spatial spectrum, resulting in inaccurate spatial spectrum estimation.

The associate editor coordinating the review of this manuscript and approving it for publication was Pavlos I. Lazaridis.

The space-time method extends one-dimensional spatial filtering to two-dimensional domain of space and time. And its two-dimensional optimization ability effectively inhibits the leakage of spectrum energy, so it still has good performance under the condition of limited time samples [5]. Frost is the most classical space-time broadband beamformer [6], which obtains the lossless output of the array normal direction signal by linearly constrained minimum variance (LCMV) beamforming. However, the Frost beamformer must adjust the pre-steering delay to ensure that the desired direction signals are in the same phase at the output of each array element, but its performance will be affected by the precision of the pre-steering delay [7]. Because it is difficult and expensive to realize high-precision pre-steering delay, a new set of linear constraints is proposed in documents [8], [9], [10] to eliminate pre-steering delay. However, the proposed linear constraint set consumes a large number of degrees of freedom (DOF) of the beamformer in advance, and when the degree of freedom consumption of desired signal is lower than that of the linear constraints, the degree of freedom is wasted. In addition, the beam response performance of these LCMV space-time broadband beamformers without pre-steering delay depends on the spatial reference point [11], and the algorithm stability is poor. In adaptive array Doppler processing, Brennan proposed an MVDR algorithm based on space-time covariance matrix [12], which can avoid the early loss of DOF and has good stability when applied to broadband spatial spectrum estimation. However, the space-time MVDR (STMVDR) algorithm is very sensitive to frequency and angle. High sensitivity to angle is an advantage, which can improve the angular resolution of spatial spectrum estimation, but high sensitivity to frequency will lead to some new problems: Due to the high sensitivity of STMVDR beamformers to frequency errors, the signal that are not at the frequency spectrum calculation grid point are suppressed as interference. That is, there is the problem of frequency mismatch. In order to avoid frequency mismatch, the STMVDR algorithm applied to broadband spatial spectrum estimation usually adopt a small enough frequency spectrum calculation interval to ensure that all frequency signals can be detected. However, this leads to the high computational complexity of the algorithm, which can not meet the requirements of real-time signal processing.

Broadband spatial spectrum estimation algorithms typically deal with two types of classical broadband signals: broadband signals consisting of multiple narrowband signals with different frequencies and broadband signals with a flat spectrum. When dealing with broadband signals with flat spectrum distribution, STMVDR algorithm can still obtain accurate spatial spectrum estimation results with the help of the remaining signals located at the frequency calculation grid point, even if there is a frequency mismatch. However, when dealing with broadband signals consisting of multiple narrowband signals of different frequencies, the frequency mismatch problem may result in failure to detect narrowband signals that are not at the frequency calculation grid point.

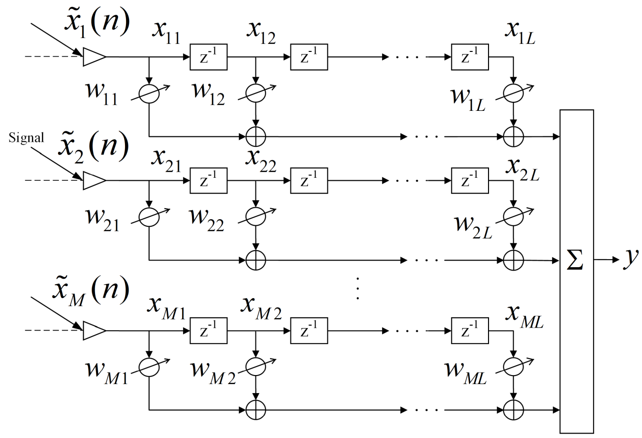

FIGURE 1. The basic array structure of STMVDR beamformer.

Derivative constraint can reduce the sensitivity of beam response to selected parameters by limiting the parameter derivative in beam response or output power function to zero [13], [14], [15]. In order to solve the problem of frequency mismatch causing the STMVDR algorithm to fail to detect narrowband signals that are not at the grid point of frequency calculation, a broadband spatial spectrum estimation method based on STMVDR and frequency derivative constraints is proposed in this paper. Firstly, based on the beam response of STMVDR beamformer, the construction method of arbitrary order frequency derivative constraint is deduced. Secondly, combining gain constraint and frequency derivative constraint, the linear constrained minimum variance problem for solving the optimal weight of the beamformer is established, and the calculation method of broadband spatial spectrum is derived. Finally, the computational complexity of the algorithm is analyzed. Numerical simulations show that, compared with space-frequency MVDR (SFMVDR) beamformer, the broadening of the frequency spectrum main lobe does not cause the shift of the peak in the true direction in the spatial spectrum. When dealing with the problem of spatial spectrum estimation of broadband signals composed of multiple narrowband signals, the proposed method can reduce the computational complexity of the algorithm by more than half, and the angular resolution and estimation accuracy of the algorithm are not obviously lost.

II. SIGNAL MODEL

Fig. 1 shows the basic processing structure of the STMVDR beamformer without pre-steering delay structure [12]. Consider the number of sensors to be M. Connect a tapped delay line of length L after each sensor. The received signal of each array element is the resolved signal after quadrature demodulation. The input broadband resolved signal of the sensor channel at the nth data sample is $\tilde{x}_1(n), \tilde{x}_2(n), \ldots, \tilde{x}_M(n)$. x_{ml} is the input data for each tap, w_{ml} is the complex weighting factor of each tap, where $m = 1, 2, \ldots, M, B, l = 1, 2, \ldots, L$. The output of the beamformer can be expressed as

$$y = \sum_{m=1}^{M} \sum_{l=1}^{L} \boldsymbol{w}_{ml} \boldsymbol{x}_{ml} \tag{1}$$

which is expressed in vector form as

$$y = \boldsymbol{w}^H \boldsymbol{x} \tag{2}$$

where,

$$\boldsymbol{w} = [w_{11}, \ldots, w_{1L}, w_{21}, \ldots, w_{2L}, \ldots, w_{M1}, \ldots, w_{ML}]^T \tag{3}$$

is the vector of ML dimensional weight coefficients,

$$\boldsymbol{x} = [x_{11}, \ldots, x_{1L}, x_{21}, \ldots, x_{2L}, \ldots, x_{M1}, \ldots, x_{ML}]^T \tag{4}$$

is the ML dimensional input data vector. For the case where the array data are generalized smooth in time, the data covariance matrix can be estimated as

$$\hat{\boldsymbol{R}} = \frac{1}{K} \sum_{k=1}^{K} \boldsymbol{x}_k \boldsymbol{x}_k^H \tag{5}$$

where, $\boldsymbol{x}_k$ denotes the k-th snap data of the estimated data covariance matrix. K denotes the number of snaps required to estimate the data covariance matrix.

The optimal weights of the STMVDR beamformer can be found by the following linearly constrained minimum variance problem

$$\begin{cases} \min P_{out} = \boldsymbol{w}^H \hat{\boldsymbol{R}} w \\ \text{s.t. } \boldsymbol{w}^H \boldsymbol{a}(\theta_0, f_0) = 1 \end{cases} \tag{6}$$

$\boldsymbol{a}$ is a space-time two-dimensional steering vector and can be written as

$$\boldsymbol{a}(\theta_0, f_0) = \boldsymbol{S}_s(\theta_0, f_0) \otimes \boldsymbol{S}_t(f_0) \tag{7}$$

where, θ_0 denotes the orientation of the signal; f_0 denotes the frequency of the signal; $\otimes$ denotes the Kronecker product; $\boldsymbol{S}_t(f_0)$ and $\boldsymbol{S}_s(\theta_0, f_0)$ denotes the L-dimensional frequency steering vector and the M-dimensional space steering vector, respectively, and the expressions are given by the following equations

$$\begin{aligned} \boldsymbol{S}_t(f_0) &= \left[1, e^{-j2\pi f_0 T_s}, \cdots, e^{-j2\pi f_0 (L-1) T_s}\right]^T \\ \boldsymbol{S}_s(\theta_0, f_0) &= \left[e^{-j2\pi f_0 \tau_1(\theta_0)}, e^{-j2\pi f_0 \tau_2(\theta_0)}, \cdots, e^{-j2\pi f_0 \tau_M(\theta_0)}\right]^T \end{aligned} \tag{8}$$

where j denotes imaginary units; T_s denotes the sampling interval of data samples; $\tau_m(\theta_0)$ denotes the propagation delay of the m-th sensor with respect to the first sensor when the source orientation is θ_0.

III. PROPOSED METHOD

A. FREQUENCY DERIVATIVE CONSTRAINT

In this section, a frequency derivative constraint on the beam response is imposed on the STMVDR beamformer to reduce the sensitivity of the beamformer to frequency. The beam response of the STMVDR beamformer at the location (θ_0, f_0) can be expressed as

$$b(\theta_0, f_0) = \boldsymbol{w}^H \boldsymbol{a}(\theta_0, f_0) \tag{9}$$

The α order frequency derivative constraint requires that the α order derivative of the beamformer's beam response at (θ_0, f_0) with respect to frequency is zero, which can be expressed as

$$\boldsymbol{w}^H \left. \frac{\partial^\alpha \boldsymbol{a}(\theta_0, f)}{\partial f^\alpha} \right|_{f=f_0} = 0 \tag{10}$$

Substituting (7) into (10) yields

$$\begin{aligned} \frac{\partial^\alpha \boldsymbol{a}(\theta_0, f)}{\partial f^\alpha} &= \frac{\partial^\alpha [\boldsymbol{S}_s(\theta_0, f) \otimes \boldsymbol{S}_t(f)]}{\partial f^\alpha} \\ &= \sum_{k=0}^{\alpha} C_\alpha^k \left[\frac{\partial^{\alpha-k} \boldsymbol{S}_s(\theta_0, f)}{\partial f^{\alpha-k}} \otimes \frac{\partial^k \boldsymbol{S}_t(f)}{\partial f^k}\right] \end{aligned} \tag{11}$$

where

$$C_\alpha^k = \frac{\alpha!}{k!(\alpha-k)!} \tag{12}$$

and

$$\begin{aligned} \frac{\partial^{\alpha-k} \boldsymbol{S}_s(\theta_0, f)}{\partial f^{\alpha-k}} &= \begin{cases} \boldsymbol{S}_s(\theta_0, f) & \alpha - k = 0 \\ -j2\pi \boldsymbol{A}^{\alpha-k} \boldsymbol{S}_s(\theta_0, f) & \alpha - k \neq 0 \end{cases} \\ \boldsymbol{A} &= diag(\boldsymbol{\tau}_1(\theta_0), \boldsymbol{\tau}_2(\theta_0), \cdots, \boldsymbol{\tau}_M(\theta_0)) \end{aligned} \tag{13}$$

and

$$\begin{aligned} \frac{\partial^k \boldsymbol{S}_t(f)}{\partial f^k} &= \begin{cases} \boldsymbol{S}_t(f) & k = 0 \\ -j2\pi \boldsymbol{B}^k \boldsymbol{S}_t(f) & k \neq 0 \end{cases} \\ \boldsymbol{B} &= diag(0, T_s, \cdots, (L-1) T_s) \end{aligned} \tag{14}$$

where $diag(\cdot)$ denotes the diagonal matrix. Then the α order frequency derivative constraint of the beam response of the weight vector at (θ_0, f_0) with respect to frequency can be expressed as

$$\boldsymbol{w}^H \sum_{k=0}^{\alpha} C_\alpha^k \left[\boldsymbol{A}^{\alpha-k} \boldsymbol{S}_s(\theta_0, f_0) \otimes \boldsymbol{B}^k \boldsymbol{S}_t(f_0)\right] = 0 \tag{15}$$

where $\boldsymbol{A}^0 = \boldsymbol{I}_{M \times M}$, $\boldsymbol{B}^0 = \boldsymbol{I}_{L \times L}$, $\boldsymbol{I}$ denotes the unit matrix.

B. BROADBAND SPATIAL SPECTRUM ESTIMATION METHOD

Setting frequency derivative constraints should follow: when using high-order frequency derivative constraints, all low-order frequency derivative constraints should be adopted [14].

Construction of linear constrained minimum variance problems based on STMVDR and frequency domain derivative constraints

$$\begin{cases} \min & P_{out} = \boldsymbol{w}^H \hat{\boldsymbol{R}} w \\ \text{s.t.} & \boldsymbol{C}(\theta_0, f_0)^H \boldsymbol{w} = \boldsymbol{G} \end{cases} \tag{16}$$

where $\boldsymbol{C}(\theta_0, f_0) = [\boldsymbol{c}_1, \boldsymbol{c}_2, \cdots, \boldsymbol{c}_J]$ is the constraint matrix at the desired response point (θ_0, f_0), c_j $(j = 1, \cdots, J)$ is the corresponding constraint vector, and $\boldsymbol{G} = [g_1, g_2, \cdots, g_J]$ is the corresponding gain response vector. The optimal weight vector satisfying (16) is

$$\boldsymbol{w}_{opt}(\theta_0, f_0) = \hat{\boldsymbol{R}}^{-1} \boldsymbol{C}(\theta_0, f_0) \left(\boldsymbol{C}^H(\theta_0, f_0) \hat{\boldsymbol{R}}^{-1} \boldsymbol{C}(\theta_0, f_0) \right)^{-1} \boldsymbol{G} \tag{17}$$

Select $\boldsymbol{c}_1 = \boldsymbol{a}(\theta_0, f_0)$ and $g_1 = 1$ to control the unit gain of the selected response point. The remaining constraint vector is the frequency derivative constraint and $\boldsymbol{c}_j$ $(j = 2, \cdots, J)$ is chosen to be the $j - 1$ order frequency derivative constraint vector, which can be expressed as

$$\boldsymbol{c}_j = \sum_{k=0}^{j-1} C_{j-1}^k \left[\boldsymbol{A}^{j-1-k} \boldsymbol{S}_s(\theta_0, f_0) \otimes \boldsymbol{B}^k \boldsymbol{S}_t(f_0) \right] (j = 2, \cdots, J) \tag{18}$$

the corresponding gain response is $g_j = 0 \, (j = 2, \cdots, J)$.

The angle-frequency two-dimensional power spectrum of the beamformer output is obtained from (17) as

$$\hat{P}(\theta_p, f_q) = \boldsymbol{G}^H \left(\boldsymbol{C}^H(\theta_p, f_q) \hat{\boldsymbol{R}}^{-1} \boldsymbol{C}(\theta_p, f_q) \right)^{-1} \boldsymbol{G} \quad (p = 1, 2, \cdots, P; q = 1, 2, \cdots, Q) \tag{19}$$

where P and Q denote the number of angle scan points and frequency scan points, respectively. To obtain an estimate of the spatial spectrum of a broadband target, the angle-frequency two-dimensional power spectrum of the beamformer output can be averaged cumulatively in the frequency dimension. The spatial spectrum of the broadband target can be expressed as

$$\hat{P}_{out}(\theta_p) = \frac{1}{Q} \sum_{q=1}^{Q} \boldsymbol{G}^H \left(\boldsymbol{C}^H(\theta_p, f_q) \hat{\boldsymbol{R}}^{-1} \boldsymbol{C}(\theta_p, f_q) \right)^{-1} \boldsymbol{G} \quad (p = 1, 2, \cdots, P; q = 1, 2, \cdots, Q) \tag{20}$$

C. FREQUENCY SCAN INTERVAL

The beamformer needs to select the appropriate frequency scan interval $\Delta f = f_q - f_{q-1}$ to ensure that the attenuation of all signals in the angle-frequency 2-dimensional power spectrum does not exceed 3 dB. Defines the standard frequency spectrum as the projection of the angular-frequency 2-dimensional power spectrum of the beamformer in the frequency-power plane for a single narrowband signal input. The frequency scan interval can be set to the 3 dB main lobe width of the standard frequency spectrum.

TABLE 1. Primary computation complexity of the algorithms under different order derivative constraints.

Algorithms	Primary computation complexity
STMVDR[16]	$O\left\{(ML)^3 + PQ\left[(ML)^2 + ML\right]\right\}$
STMVDR+1st	$O\left\{(ML)^3 + \frac{2}{\eta_1} PQ\left[(ML)^2 + ML\right]\right\}$
STMVDR+1st+2nd	$O\left\{(ML)^3 + \frac{3}{\eta_2} PQ\left[(ML)^2 + ML\right]\right\}$
STMVDR+1st+2nd+ …+*i*-order	$O\left\{(ML)^3 + \frac{(i+1)}{\eta_i} PQ\left[(ML)^2 + ML\right]\right\}$

D. COMPUTATIONAL COMPLEXITY ANALYSIS

The computational complexity of the spatial spectrum estimation algorithm depends on the number of frequency spectrum scan points. The number of frequency spectrum scan points is minimized when the maximum frequency calculation interval of the algorithm is the 3 dB main lobe width of the standard frequency spectrum. Table 1 statistically shows the main computational complexity (number of complex multiplications) of different algorithms when the minimum number of frequency computation points is selected. Where P and Q represent the minimum values of angle scan points and frequency scan points of the angle-frequency 2-dimensional power spectrum scan grid of STMVDR algorithm, respectively; $\eta_i \, (i = 1, 2, \cdots N)$ denotes the ratio of the minimum number of frequency scan points between the STMVDR algorithm and the spatial spectrum estimation algorithm based on STMVDR and the i-order derivative constraint. The computational complexity of calculating the derivative constraint vector in Section III, paragraph A, is not considered in the table, because it can be pre-calculated and stored in the computing device. Since the derivative constraint extends the 3 dB main lobe width of the standard frequency spectrum, it is possible to reduce the minimum value of the number of points calculated for the algorithm frequency. From Table 1, it can be found that the computational complexity of the spatial spectrum estimation algorithm based on STMVDR and the i-order derivative constraint is lower than that of STMVDR algorithm when $\eta_i > i + 1$.

IV. SIMULATION ANALYSIS

In this section, numerical simulations are provided to demonstrate the effectiveness and performance advantages of the proposed method. The highest order of the derivative constraint used in the simulation is second order. The comparison algorithms are spatial spectrum estimation method based on STMVDR and the spatial spectrum estimation method based on STMVDR. Among them, the space-frequency MVDR method decomposes subbands through FFT, and then carries out the spatial spectrum estimation algorithm based on MVDR in each subband.

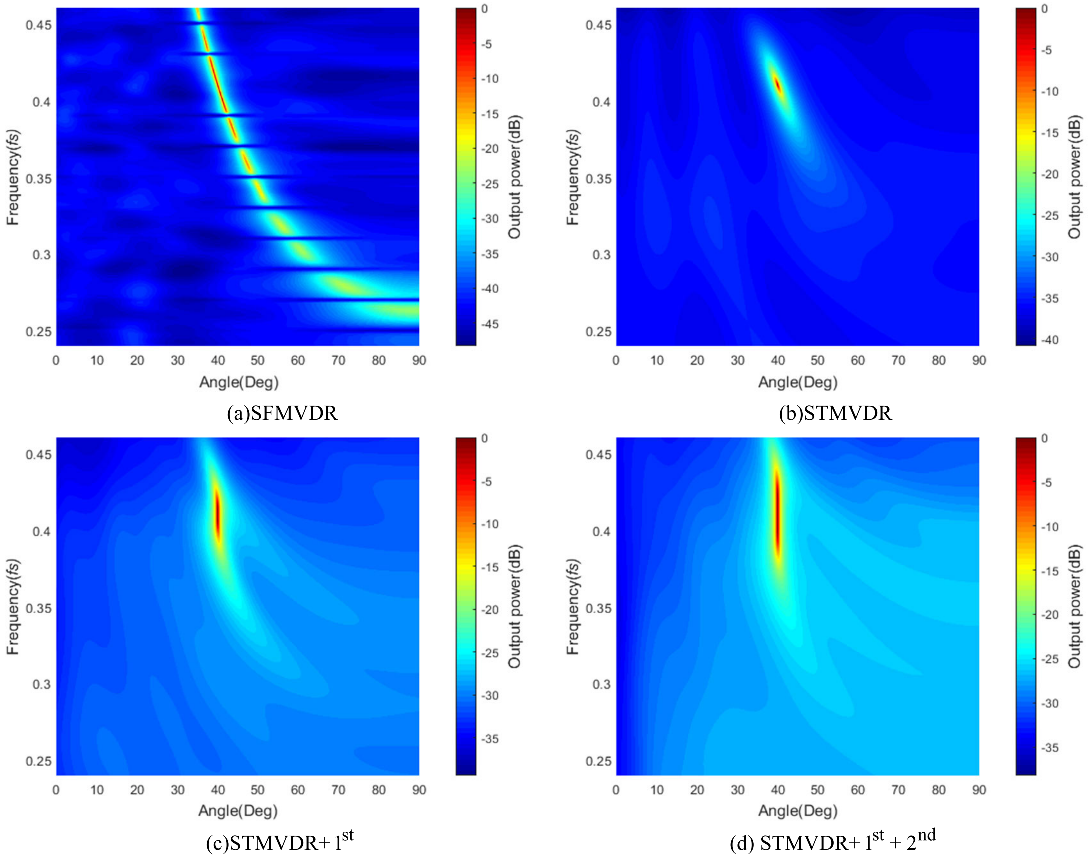

FIGURE 2. Angle-frequency 2-dimensional power spectrum of the algorithms.

Considering a 16 yuan uniform linear array, the STMVDR method connects a 5-tap delay line structure at each array unit. The space-frequency MVDR (SFMVDR) method uses only 50 data points and decomposes the sub-band based on FFT. The number of snapshots of STMVDR method and SFMVDR method is 2 ML and 2 M, respectively, and the snapshot overlap rate is 0% and 50%, respectively, so the data consumption of the two algorithms to estimate the data covariance is almost the same. Assuming working in a broadband environment, the array spacing is equal to half a wavelength of the maximum frequency component. The sampling frequency f_s is equal to twice the maximum frequency, and the processing bandwidth of the expanded beamformer is from $0.24f_s$ to $0.46f_s$.

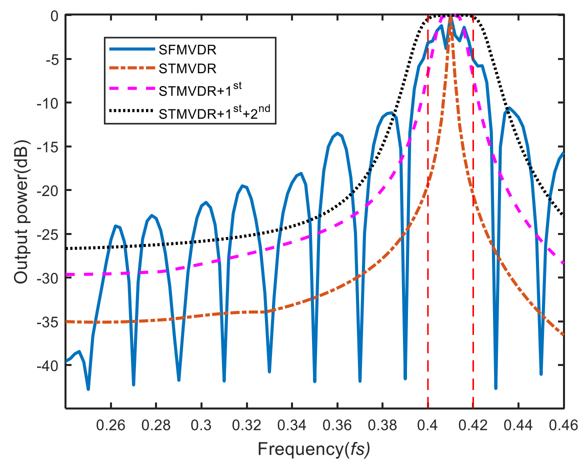

FIGURE 3. The standard frequency spectrum of the algorithms.

A. THE STANDARD FREQUENCY SPECTRUM

Consider a narrow-band signal with a frequency of $0.41f_s$ from a 40° hitting the array. Four algorithms (SFMVDR method, STMVDR method, STMVDR combined with first derivative constraint, STMVDR combined with first derivative constraint and second derivative constraint) are used to obtain the angle-frequency 2-dimensional power spectrum as shown in Fig. 2, and the angle interval and frequency interval of the angle - frequency 2-dimensional power spectrum scan grid are selected as 0.1 degree and $0.002f_s$ respectively.

Fig. 3 shows the standard frequency spectrum of the four algorithms. Due to the lack of frequency domain optimization ability, the SFMVDR method will produce spectrum leakage in short snapshot duration, resulting in wide main lobe and high sidelobe, as shown in Fig. 3. Although the SFMVDR method has a wide frequency spectrum main lobe, the leaked frequency energy points to an angle different from

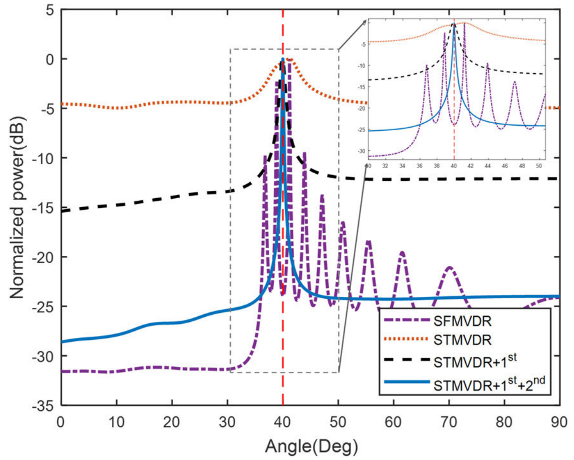

FIGURE 4. Spatial spectrum of the algorithms with narrowband signal input.

the true incoming signal direction as shown in Fig. 2(a). STMVDR method has the ability of two-dimensional optimization of spatial frequency at the same time, so as shown in Fig. 2 (b) and Fig. 3, sharp peak is formed in both angle and frequency. The main lobe of the standard frequency spectrum is expanded by STMVDR with frequency derivative constraint, and the spatial spectrum peak of the expanded frequency still points to the arrival direction of true signal, as shown in Fig. 2 (c) and (d). In addition, STMVDR combines the first derivative constraint and the second derivative constraint at the same time, and obtains a wider expansion of the standard frequency spectrum main lobe than only combining the first derivative constraint, as shown in Fig. 3, and the correlation peak is not shifted.

B. FREQUENCY MISMATCH PROBLEM

Considering that a narrow-band signal with a frequency of $0.41f_s$ affects the array from 40°, the frequency calculation interval of the calculation grid is increased to $0.02f_s$. The frequency $0.41f_s$ of the narrowband signal is just between the frequency calculation points $0.40f_s$ and $0.42f_s$, so the frequency of the grid calculation point will not match the actual frequency. In Fig. 4, the broadband spatial spectra of these four algorithms is compared. As shown in Fig. 4, the beam patterns of the two proposed algorithms all point to the true direction of arrival. In addition, compared with the STMVDR algorithm which only combines the first derivative constraint, the STMVDR algorithm which combines the first derivative constraint and the second derivative constraint simultaneously obtains sharper beam pointing and lower side-lobe level. The beam patterns of STMVDR algorithm and SFMVDR algorithm do not point to the actual direction of arrival, as shown in Fig.4. The main lobe width of the standard frequency spectrum of the STMVDR algorithm is narrow. At two grid points $0.40f_s$ and $0.42f_s$ adjacent to the actual signal frequency $0.41f_s$, the frequency response has been greatly attenuated, as shown in Fig. 3, so its spatial spectrum

TABLE 2. Running time when the maximum frequency calculation interval is selected.

Algorithms	Maximum frequency calculation interval	Number of frequency calculation points Q	Running time
STMVDR	$0.002\ f_s$	111	1.8590 s
STMVDR+1st	$0.01\ f_s$	23	0.9419 s
STMVDR+1st+2nd	$0.024\ f_s$	10	0.8376 s

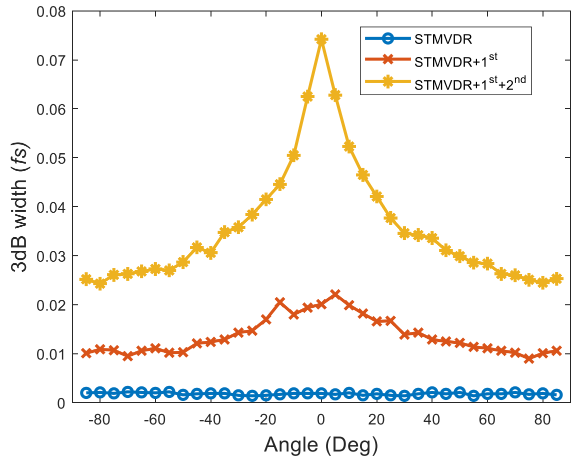

FIGURE 5. 3dB main lobe width of the standard frequency spectrum at different angles.

has a wide main lobe and a high side lobe. Although the frequency spectrum main lobe width of SFMVDR algorithm is wide, the spectral energy leakage of the actual signal at the frequency calculation point will only lead to the beam pointing error.

C. ALGORITHM COMPLEXITY ANALYSIS

Fig. 5 shows the 3dB main lobe width of the standard frequency spectrum at different angles. It can be found that the 3dB main lobe width of the standard frequency spectrum of STMVDR algorithm is the narrowest. The 3dB main lobe width of the standard frequency spectrum is expanded by increasing the frequency derivative constraint, and a wider 3dB main lobe width can be obtained by combining the first-order-frequency derivative constraint and the second-order-frequency derivative constraint than only combining the first - order frequency derivative constraint. The frequency calculation range of the algorithm can be selected according to the 3dB main lobe width of the standard frequency spectrum. Under the case of equal interval, the maximum frequency calculation interval should be the minimum of the main lobe width of the standard frequency spectrum of 3dB. Table 2 shows the running time of different algorithms on the same computer using Matlab R2018b and 2.6 GHz CPU when the maximum frequency calculation interval is chosen, and it can be found that the proposed algorithm reduces the running

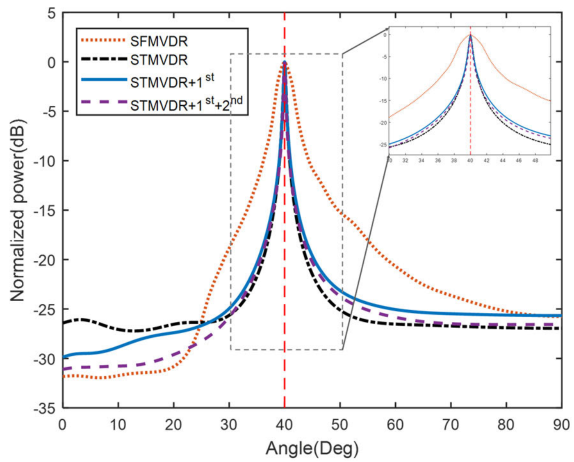

FIGURE 6. Spatial spectrum under multiple narrowband signal inputs.

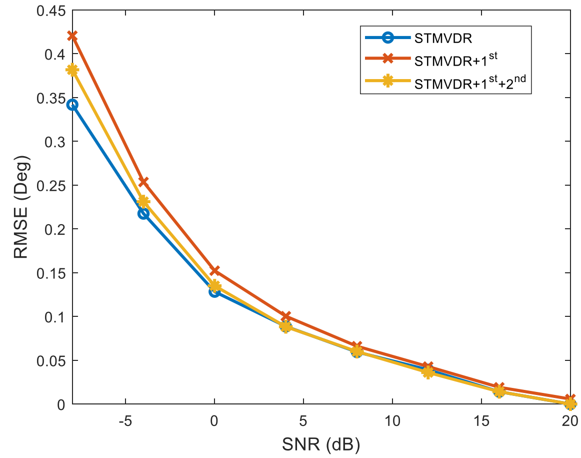

FIGURE 7. RMSE of spatial spectrum estimation with different SNR.

time by more than half. In addition, the width of the 3dB main lobe of the Under the case of equal interval, the maximum frequency calculation interval should be the minimum of the 3dB main lobe width of the standard frequency spectrum. increases with the decrease of the angle, which is obvious, so the frequency calculation interval at small angles can be further increased to reduce the computational complexity of the algorithm.

D. ANGULAR RESOLUTION OF THE ALGORITHM

The angular resolution of the algorithms are evaluated by comparing the width of the main lobe of the spatial spectrum. Assume a broadband signal impingement array consisting of four narrowband signals with frequencies $0.30f_s$, $0.32f_s$, $0.35f_s$ and $0.41f_s$ respectively from 40°, and the frequency calculation interval is chosen according to Table 2. Fig. 6 illustrates the comparison results of the spatial spectra of the four algorithms with multiple narrowband signal inputs. As shown in Fig. 6, the spatial spectrum estimation algorithm based on STMVDR and frequency derivative constraints is basically the same as the STMVDR algorithm in terms of the main lobe width. Therefore, after increasing the frequency calculation interval, the proposed algorithm can still obtain an angular resolution comparable to that of the STMVDR algorithm. SFMVDR algorithm has no time domain optimization ability, and the spectrum leakage will lead to beam pointing error, so its beam main lobe is the widest.

E. ROOT MEAN SQUARE ERROR

Fig. 7 evaluates the relationship between the root mean square error (RMSE) of spatial spectrum estimation and the change of signal-to-noise ratio (SNR) of different algorithms. The RMSE of spatial spectrum estimation is estimated by 300 independent Monte Carlo simulations. The simulation conditions are consistent with paragraph D. It can be seen that the RMSEs of the proposed algorithm are slightly higher than those of the STMVDR algorithm at low SNR, but at high SNR, the RMSEs curves of the proposed algorithm almost overlap with those of the STMVDR algorithm.

V. CONCLUSION

In order to reduce the sensitivity of STMVDR to frequency errors, this paper extends the main lobe of the standard frequency spectrum of STMVDR beamformer by adding a frequency derivative constraint. When the broadband signal received by the array consists of multiple narrowband signals of different frequencies, the proposed method can reduce the computational complexity of the algorithm by more than half by reducing the frequency computation density of the broadband beamformer, and there is no significant loss in the angular resolution and estimation accuracy of the algorithm. However, since adding frequency derivative constraints consumes additional DOF of the beamformer, the proposed algorithm may lose some degree of spatial spectral estimation performance when the broadband signal received by the array consumes a high amount of DOF (e.g., a broadband signal with a flat spectrum).

REFERENCES

[1] W. Liu and S. Weiss, *Wideband Beamforming: Concepts and Techniques*. Hoboken, NJ, USA: Wiley, 2010.

[2] L. C. Godara, "Application of the fast Fourier transform to broadband beamforming," *J. Acoust. Soc. Amer.*, vol. 98, no. 1, pp. 230–240, Jul. 1995.

[3] G. Su and M. Morf, "The signal subspace approach for multiple wideband emitter location," *IEEE Trans. Acoust., Speech, Signal Process.*, vol. ASSP-31, no. 6, pp. 1502–1522, Dec. 1983.

[4] H. Wang and M. Kaveh, "Coherent signal-subspace processing for the detection and estimation of angles of arrival of multiple wide-band sources," *IEEE Trans. Acoust., Speech, Signal Process.*, vol. ASSP-33, no. 4, pp. 823–831, Aug. 1985.

[5] R. T. Compton Jr., "The relationship between tapped delay-line and FFT processing in adaptive arrays," *IEEE Trans. Antennas Propag.*, vol. AP-36, no. 1, pp. 15–26, Jan. 1988.

[6] O. L. Frost, "An algorithm for linearly constrained adaptive array processing," *Proc. IEEE*, vol. 60, no. 8, pp. 926–935, Aug. 1972.

[7] S. Zhang and I. L. J. Thng, "Robust presteering derivative constraints for broadband antenna arrays," *IEEE Trans. Signal Process.*, vol. 50, no. 1, pp. 1–10, Jan. 2002.

[8] K. Buckley, "Spatial/spectral filtering with linearly constrained minimum variance beamformers," *IEEE Trans. Acoust., Speech, Signal Process.*, vol. ASSP-35, no. 3, pp. 249–266, Mar. 1987.

[9] L. C. Godara and M. R. S. Jahromi, "Convolution constraints for broadband antenna arrays," *IEEE Trans. Antennas Propag.*, vol. 55, no. 11, pp. 3146–3154, Nov. 2007.

[10] R. Ebrahimi and S. R. Seydnejad, "Elimination of pre-steering delays in space-time broadband beamforming using frequency domain constraints," *IEEE Commun. Lett.*, vol. 17, no. 4, pp. 769–772, Apr. 2013.

[11] Y. Wang, H. Xu, B. Wang, and M. Sun, "Optimal array phase center study for frequency-domain constrained space-time broadband beamforming," *IEEE Access*, vol. 11, pp. 1295–1305, 2023, doi: 10.1109/ACCESS.2022.3233645.

[12] L. E. Brennan and L. Reed, "Theory of adaptive radar," *IEEE Trans. Aerosp. Electron. Syst.*, vol. AES-9, no. 2, pp. 237–252, Mar. 1973.

[13] S. Applebaum and D. Chapman, "Adaptive arrays with main beam constraints," *IEEE Trans. Antennas Propag.*, vol. AP-24, no. 5, pp. 650–662, Sep. 1976, doi: 10.1109/TAP.1976.1141416.

[14] C.-C. Tseng, "Minimum variance beamforming with phase-independent derivative constraints," *IEEE Trans. Antennas Propag.*, vol. 40, no. 3, pp. 285–294, Mar. 1992.

[15] V. V. Reddy, B. P. Ng, and A. W. H. Khong, "Derivative-constrained frequency-domain wideband DOA estimation," *Multidimensional Syst. Signal Process.*, vol. 25, no. 1, pp. 211–233, Jan. 2014, doi: 10.1007/s11045-012-0201-8.

[16] F. G. Yan, M. Jin, S. Liu, and X. L. Qiao, "Real-valued MUSIC for efficient direction estimation with arbitrary array geometries," *IEEE Trans. Signal Process.*, vol. 62, no. 6, pp. 1548–1560, Mar. 2014, doi: 10.1109/TSP.2014.2298384.

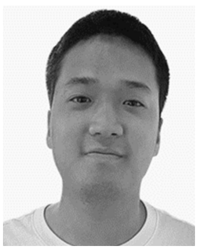

YANG WANG was born in 1996. He received the B.S. degree from Harbin Engineering University, in 2020. He is currently pursuing the M.S. degree with PLA Strategic Support Force Information Engineering University. His research interests include array signal processing and sonar signal processing.

HAIYUN XU received the M.S. and Ph.D. degrees from National Digital Switching System Engineering and Technological Research Center (NDSC), Zhengzhou, China, in 2019 and 2022, respectively. He is currently with PLA Strategic Support Force Information Engineering University, China, where he was involved in communications and information systems. His main research interests include array signal processing and parameter estimation.

BIN WANG received the Ph.D. degree from PLA Information Engineering University, in 2007. She is currently a Professor with PLA Strategic Support Force Information Engineering University. Her research interests include underwater acoustic communication signal processing and blind channel equalization.

MINGLEI SUN received the Ph.D. degree from the Harbin Institute of Technology, in 2015. He is currently with PLA Strategic Support Force Information Engineering University. His research interest includes array signal processing.